CONF-780228--2

MASTER

OPTIMAL DESIGN OF SEASONAL STORAGE FOR 100% SOLAR SPACE HEATING IN BUILDINGS

by

R.O. Mueller, J.G. Asbury, J.V. Caruso, D.W. Connor and R.F. Giese

Prepared for

AAAS Symposium on
Efficient Comfort Conditioning
Washington, D.C.
February 1978

U of C-AUA-USDOE

ARGONNE NATIONAL LABORATORY, ARGONNE, ILLINOIS

Operated under Contract W-31-109-Eng-38 for the

U. S. DEPARTMENT OF ENERGY

DISCLAIMER

The facilities of Argonne National Laboratory are owned by the United States Government. Under the terms of a contract (W-31-109-Eng-38) between the U. S. Department of Energy, Argonne Universities Association and The University of Chicago, the University employs the staff and operates the Laboratory in accordance with policies and programs formulated, approved and reviewed by the Association.

The facilities of Argonne National Laboratory are owned by the United States Government. Under the terms of a contract (W-31-109-Eng-38) between the U. S. Department of Energy, Argonne Universities Association and The University of Chicago, the University employs the staff and operates the Laboratory in accordance with policies and programs formulated, approved and reviewed by the Association.

To be published in the Proceedings of the AAAS Symposium on Efficient Comfort Conditioning, held at the 1978 Winter Annual Meeting in Washington D.C.

OPTIMAL DESIGN OF SEASONAL STORAGE

FOR 100% SOLAR SPACE HEATING IN BUILDINGS*

by

R.O. Mueller, J.G. Asbury, J.V. Caruso, D.W. Connor and R.F. Giese

Energy and Environmental Systems Division
Argonne National Laboratory
9700 South Cass Avenue
Argonne, Illinois 60439

*Work supported by the Division of Energy Storage Systems, and the Office of the Assistant Administrator for Conservation and Solar Applications of the U.S. Department of Energy.

/

I. INTRODUCTION

In many applications of solar energy -- space heating and cooling of buildings are two examples -- load requirements are non-zero only over a fraction of the year. In meeting these periodic loads with so-called "diurnal" solar systems, that is, systems containing storage capacities on the order of a day's supply, the solar radiation incident on the collector field during the off-season remains largely unused because of the lack of contiguous demand. This can represent a substantial opportunity loss in solar collection. Because of the capital-intensive and fuel-unintensive nature of solar technologies this hampers the economic use of solar energy in such applications. For example, in winter space heating of buildings, the fraction of solar energy that falls outside of the main winter months may reach as high as 70%. Recently, a number of solar system designs have been proposed, some built, that incorporate storage capacities on the order of one or several months supply.[1] In these "seasonal" solar schemes, solar collection can occur over a much greater fraction of the year, with energy stored for periods extending over several months or longer before being used up by the load.

By improving utilization of the available solar input over the full year, a seasonal system will reduce collector area requirements over that of a comparable diurnal system while providing the same total energy to load. The resultant savings in collector area costs represent a major economic rationale of seasonal storage. A second benefit is to lessen, or eliminate altogether, requirements for a backup energy supply and the associated problems of load management.[2] By providing a reliable, long-term buffer between short-term stochastic variations in the solar input and the load, seasonal storage permits design of solar systems that supply all, or nearly all, of the total energy requirements. Against these benefits must be weighed the added capital cost of the storage unit.

In this paper we present an analysis of seasonal solar systems that contain water as the sensible heat storage medium. A concise model is developed under the assumption of a fully-mixed, uniform temperature, storage tank that permits efficient simulation of long-term (multi-day) system performance over the course of the year. The approach explicitly neglects the effects of short-term (sub-daily) fluctuations in insolation and load, effects that will be extremely small for seasonal solar systems. Although not adequate as a detailed design tool, this approach is useful for examining the major design tradeoffs of concern in this paper. The application considered is winter space heating, although the approach adopted will be useful for other periodic loads as well.

The analysis proceeds through two stages. First, we solve for the thermal performance of seasonal solar systems that are designed to supply 100% of load without any backup, under "reference year" monthly normal ground temperature and insolation conditions. The systems are matched to the load requirements of a 150 m^2, well-insulated, detached single family dwelling unit. Although not considered here, a similar approach could be applied to partial seasonal systems, supplying less than full load requirements. For the class of 100% solar systems, it is possible to derive approximate analytic expressions that relate sizing and design requirements of the collector to the storage component. Based on these results, we estimate unit break-even costs of seasonal storage by comparing the capital and fuel costs of conventional space heating technologies against those of a seasonal solar system. At costs below the break-even estimates, the seasonal solar system has an economic advantage over the conventional system.

Seasonal solar systems designed to meet load under average "reference year" weather conditions will fall short during the later stages of more severe winters. To avoid this shortfall, either the seasonal solar system can be oversized or a small backup heating system attached. As a second step in the analysis we have made a rough comparison of the cost tradeoffs between these alternatives, by examining statistical variations in winter season conditions over the past several decades.

The four northerly sites for which detailed results are presented here are: Caribou, Maine; Madison, Wisconsin; Boston, Massachusetts; and Sterling, Virginia. Provided the storage vessel is extremely well insulated, we find substantial performance gains for the seasonal over the diurnal system, with the annual fraction of useful solar energy delivered to load greater by as much as a factor of two under reference year weather conditions. The corresponding storage break-even costs are sensitive to the values chosen for collector costs and conventional system costs, ranging from 5¢/gallon to about 15¢/gallon.

Although the storage break-even cost estimates presented here are dependent on the costs assumed for collectors and for the conventional technologies, the qualitatively low range of estimates is symptomatic of a seasonal storage system. On average, thermal energy is cycled through a seasonal storage device only about once per year, leading to relatively low annual energy throughputs. For example, for a water storage medium, cycled over a 100°F (55°C) temperature difference, the device's annual energy throughput is about 850 Btu/gal/yr (230 kJ/kg/yr). Assuming, for simplicity, the cost of input energy is zero (collectors are free), the value of a storage increment is set in this example directly by the cost of a comparably sized conventional energy source, leading to a break-even estimate of 5¢/gal for a 10% capital charge rate and for a levelized conventional energy cost of $\$6/10^6$ Btu. By contrast, in diurnal storage applications, energy is cycled through the storage device many times over the season, increasing proportionately the total energy throughput and the storage break-even cost.

The remainder of the paper is organized as follows: In Section II we present simplified storage break-even estimates for seasonal solar systems compared against diurnal systems as well as against conventional supply systems. In Section III we present a model of a seasonal solar system, that is solved in Section IV for long-term system performance using a Fourier series approach. In Section V we compare the costs of seasonal solar systems against conventional systems and develop estimates of storage break-even costs. In this final section we also consider the cost tradeoffs associated with the design of seasonal systems capable of meeting load under worst-case winter conditions.

II. STORAGE BREAK-EVEN COSTS -- SIMPLE ESTIMATES

The analysis presented in this section serves to illustrate the role of seasonal storage, while offering simple estimates of storage break-even costs under a number of simplifying assumptions. Figure 1 depicts the application of a seasonal solar system in supplying energy to meet the periodic heating load Q_L, which is assumed constant over the fraction ν of the year. By permitting collection and storage of solar energy during the "off-season", the $(1-\nu)$ remaining fraction of the year, the seasonal solar system provides a reduction in collector area relative to a comparable diurnal solar system incorporating one or several days storage capacity. For simplicity, daily insolation is here assumed constant over the year.

If the storage tank is assumed perfectly insulated, and temperature-dependent collector losses are ignored, the reduction in collector area is given by

$$\frac{A_d - A_s}{A_d} = 1-\nu \quad . \tag{1}$$

A_s and A_d are the area requirements of the seasonal and diurnal solar systems, respectively, with both systems designed to meet the full load. Losses from the seasonal storage tank during the off-season and the increasing temperature of the collector inlet temperature during the off-season will tend to increase collector area requirements A_s leading to a modification of Eq. 1. If we denote by β the fraction of off-season solar output that is actually delivered to load, the reduction in area requirements becomes

$$\frac{A_d - A_s}{A_d} = \frac{\beta(1-\nu)}{\nu + \beta(1-\nu)} \quad . \tag{2}$$

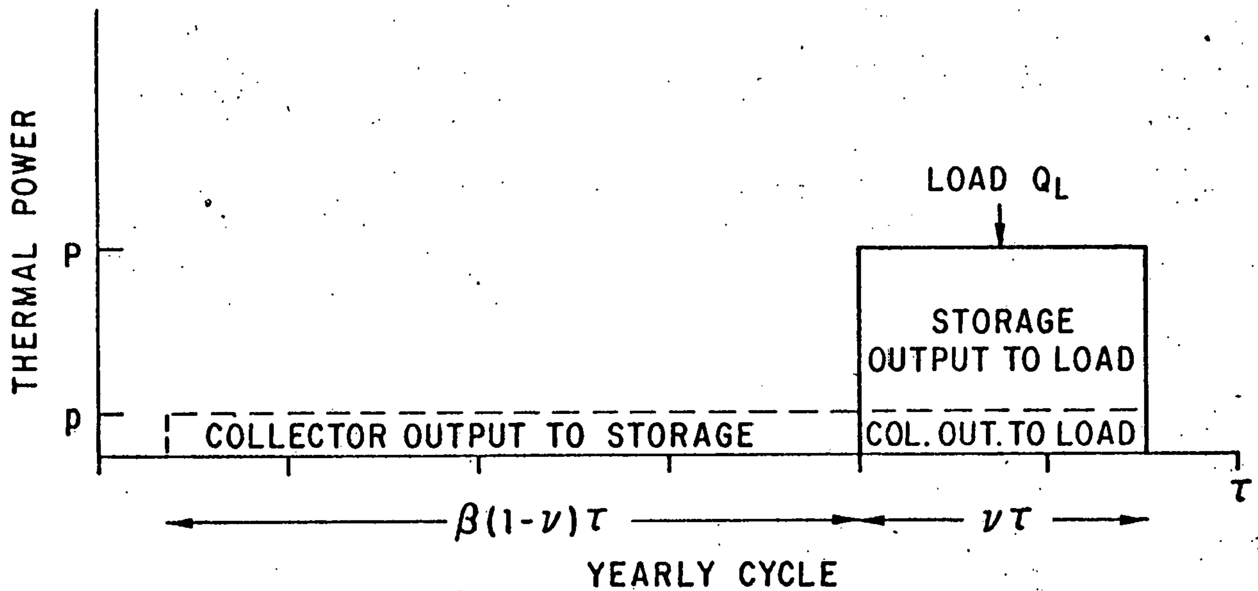

Fig. 1. Schematic of Yearly Operation of a Seasonal Solar System in Meeting Simplified Load Q_L.

The net savings in collector related costs is given by

$$\left(c_c P/p\right)\left(1 - A_s/A_d\right), \qquad (3)$$

where c_c represents unit collector costs, P the constant power requirement of the load, and p the daily average thermal power output per unit collector area, with A_d then given by P/p.

Against the net cost savings in the collector unit must be weighed the added capital cost of the storage unit. The capacity of seasonal storage that maximizes the reduction in collector area is given by

$$S = \frac{\nu\tau P}{\beta}\left(1 - A_s/A_d\right) \quad , \qquad (4)$$

where τ represents a year and S is the total stored energy at the onset of load. In Eq. 4 the β^{-1} factor accounts for the oversizing of storage needed to offset thermal losses, while the factor $(1 - A_s/A_d)$ accounts for the fraction of load met directly by collector output. Denoting the cost per unit storage capacity by c_s, the cost of the storage unit is then $c_s \cdot S$. Returns to scale on the unit cost of storage are neglected.

Equating storage costs to collector savings, and solving for c_s yields

$$\tilde{c}_s = \left(c_c/p\right)\left(\beta/\nu\tau\right) \quad . \qquad (5)$$

$\tilde{c}_s$ represents the cost of storage for which the seasonal and diurnal solar systems have equal total costs.[3]

Analogously, we can compare the economics of a seasonal solar system against a conventional heating system. The unit capital and fuel cost components of the conventional system are denoted c_{conv} and c_F, respectively, and the total annualized cost in constant dollars is given by

$$\left(c_{conv}P\right)i + c_F(\nu P\tau/\eta)L, \tag{6}$$

where i is the real capital recovery factor, L is the fuel levelization factor over the life of the device and η the conversion efficiency of the device. Equating the total annualized costs of the seasonal solar and conventional heating technologies and solving for c_s yields

$$\tilde{c}_s' = \frac{\left[c_{conv} + c_F(\nu\tau/\eta i)L\right]\left[\nu + \beta(1-\nu)\right] - c_c\nu/p}{\nu(1-\nu)\tau} . \tag{7}$$

$\tilde{c}_s'$ represents the break-even cost of seasonal storage relative to the conventional heating technology.

For a typical load of three months duration, $\nu = .25$, and an off-season storage efficiency of 80%, $\beta = .8$, collector area requirements for the seasonal system are reduced by 70%, that is $A_s = .3A_d$. Assuming an optimistic level of average power output from the collector unit of about .10 kW/m², and a collector cost of $100/m², we obtain a value of $\tilde{c}_s$ of 35¢/kWh. For sensible heat storage in water with a change in storage temperature over the heating season of 100°F, $\tilde{c}_s$ can be expressed as 8.6¢/gal. Analogously, we evaluate Eq. 7 for the storage break-even cost $\tilde{c}_s'$ against a conventional fossil-fired heating technology with cost parameters c_{conv} = $50/kW, $\eta = .55$, and c_F = 1.5¢/kWh. Assuming a real capital recovery rate of 10%, and fuel levelization factor of 2 (real fuel escalation of 4%/year over a 30 year lifetime) the value of $\tilde{c}_s'$ becomes 45¢/kWh or 11¢/gal. At zero collector-related costs, $\tilde{c}_s'$ is 65¢/kWh or 16¢/gal.

III. MODEL DESCRIPTION

A schematic of the seasonal solar system design studied in this report is given in Fig. 2. The system is assumed hydronic, with the storage medium fully mixed (isothermal) at temperature T_s. The collector and load connections are attached separately to the storage module, requiring solar energy to pass from collector to storage and then to load.[4]

Representing the instantaneous thermal power output from the collector unit by the Hottel-Whillier equation, we integrate this over the course of a day's solar charging period to obtain the total energy collected

$$\Delta Q_{col}/\Delta t = A_c F_R \left[(\tau\alpha)\ H_T - fU_L \left(\langle T_{cin} \rangle_c - \langle T_a \rangle_c \right) \right] . \qquad (8)$$

The collector specific parameters are: U_L, collector heat loss coefficient; $(\tau\alpha)$, transmittance absorptance product; F_R, collector heat removal factor; and A_C collector area. H_T is the average over the day, Δt, of solar radiation incident on the inclined collector surface. Thermal losses from the collector unit occur only during the collection period $\tilde{t} = f\Delta t$, with $\langle T_{cin} \rangle_c$ and $\langle T_a \rangle_c$ representing the average of collector inlet temperature and ambient temperature during this period. In applying Eq. 8 to a seasonal solar system, the analysis is simplified considerably by approximating $\langle T_{cin} \rangle_c$ by the storage temperature T_s at the onset of the collection period. For a seasonal system this represents a reasonable approximation since total storage heat capacities are sized well above daily collector and load heat requirements, and where as a result, changes in storage temperatures over a day are small, generally less than a few degrees Centigrade.

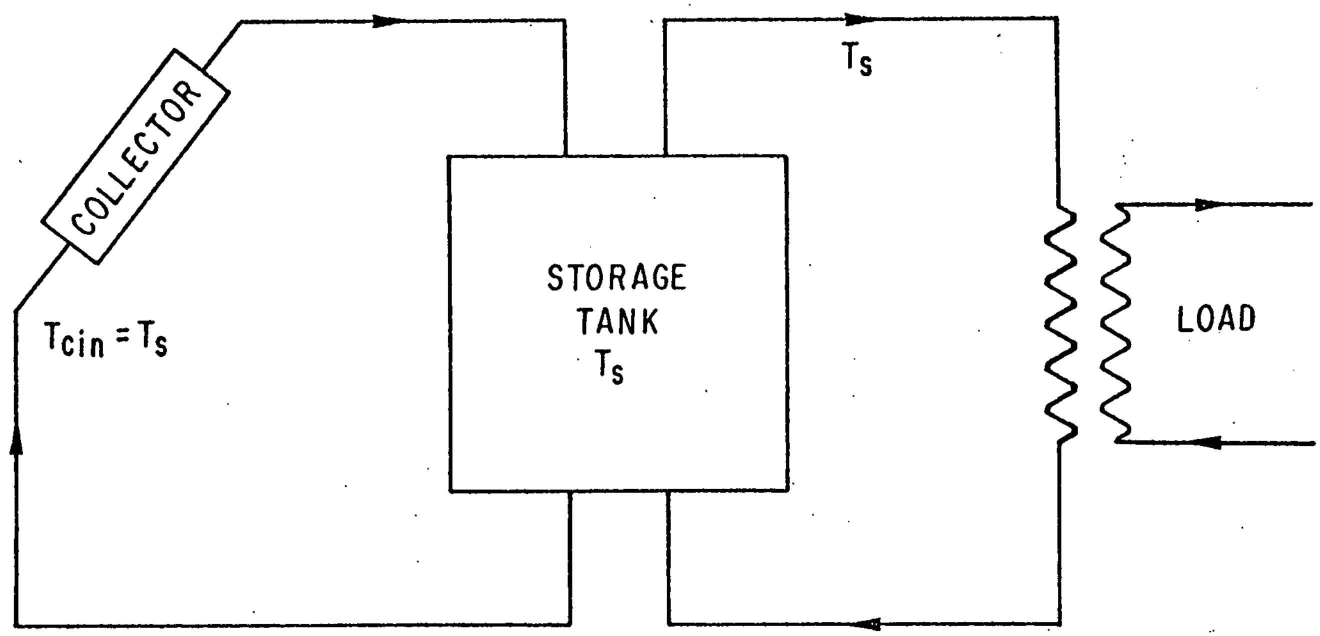

Fig. 2. Schematic of a Seasonal Solar System Containing a Fully Mixed Storage Medium

To simplify notation, we recast Eq. 8 by combining (for a specific collector type) insolation and ambient temperature into a single variable, the stagnation temperature,

$$T_c = U_c^{-1}(\tau\alpha)H_T + \langle T_a \rangle_c \quad , \tag{9}$$

when $U_c = fF_RU_L$. T_c is formally equal to the value of collector inlet temperature for which heat collection goes to zero. Using Eq. 9, and setting $\langle T_{cin} \rangle_c$ equal to T_s, Eq. 8 becomes

$$\Delta Q_{col}/\Delta t = A_cU_c(T_c - T_s) \quad , \tag{10}$$

applicable for $T_s<T_c$. In the fall and early winter seasons lower ambient temperatures and insolation levels cause T_c to decrease, and T_s may actually exceed T_c for brief periods until load requirements lower storage temperatures sufficiently. During this period collectors are assumed not to operate, and ΔQ_{col} is set equal to zero.

The total daily load requirement during the heating season is represented exogenously by

$$\Delta Q_{load}/\Delta t = A_\ell U_\ell T_\ell \tag{11}$$

valid for $T_\ell>0$; ΔQ_{load} being set to zero for $T_\ell \leq 0$. T_ℓ is an effective daily average temperature difference between heated space and ambient, A_ℓ is the total area of the building shell, and U_ℓ the average heat loss coefficient of the structure. Although, in principle, Eq. 11 can represent all or only a fraction of a building's daily load (with the remainder made up by a conventional heating system), the analysis below assumes ΔQ_{load} to be the full load requirement. Within the simple degree-day approach adopted here, T_ℓ reduces to $T_r - \langle T_a \rangle$, with T_r the constant room temperature setting and $\langle T_a \rangle$ the daily average ambient temperature.

We bypass the complication of defining a load heat-exchanger equation, by assuming that the seasonal solar system is always capable of meeting the load requirements specified by Eq. 11. Implicit in this approach are the assumptions that: (1) the load heat-exchanger is sized adequately to meet design heating conditions and (2) throughout the winter season storage temperatures remain above a minimum value adequate for space heating purposes. The solutions presented in the next section are explicitly required to satisfy the latter assumption.

Besides thermal output to load, inevitable tank losses can represent a substantial (undesirable) thermal drain on the storage unit, occurring year-round. We represent these losses by

$$\Delta Q_{loss}/\Delta t = A_s U_s T_{loss} \quad , \tag{12}$$

with T_{loss} an effective daily average temperature difference between the storage tank and its surrounding environment. U_s is the average heat transfer coefficient for the storage tank and A_s is the tank surface area, with A_s roughly proportional to the 2/3 power of tank volume V_s. Although unlikely to occur in a space heating application, the storage medium can gain energy from its surroundings provided T_{loss} is negative. In the present analysis we assume the storage vessel is buried underground, and approximate T_{loss} by the simple temperature difference $T_s - T_g$, with the ground temperature, T_g, constant and independent of T_s.[5] The corresponding value of U_s in Eq. 12 is taken to include the composite thermal resistance of tank insulation and surrounding earth.

Balancing the net of daily thermal inputs and outputs to the storage unit, to the change in its internal sensible energy leads to an equation defining the daily change in tank temperature

$$V_s \rho c_p \Delta T_s / \Delta t = \left(\Delta Q_{col} - \Delta Q_{load} - \Delta Q_{loss}\right) / \Delta t \quad , \tag{13}$$

with ρ the storage mass density and c_p its specific heat. With substitution of Eqs. 10-12, and rearrangement of terms, Eq. 13 can be written

$$\frac{\Delta T_s}{\Delta t} + \left(\lambda_c + \lambda_s\right) T_s = \lambda_s T_g + \lambda_c T_c - \lambda_\ell T_\ell \quad , \tag{14}$$

where the λ's are component time constants defined by: $\lambda_i = A_i U_i / V_s \rho c_p$. Eq. 14 forms the basic defining equation of system performance that can be applied to both 100% and partial seasonal solar systems. Given knowledge of the temperature variables $T_c(t)$ and $T_\ell(t)$, and an initial value for $T_s\left(t_o\right)$, the solution for $T_s(t)$ can be obtained directly using a numerical finite difference approach. An alternate approach, adopted in the following section, is to develop a Fourier-series representation for T_s that hinges upon the roughly periodic behavior of the driving temperatures T_c and T_ℓ.

IV. SYSTEMS ANALYSIS

This section presents an analysis of system performance, via Eq. 14, under the assumptions that: (1) the seasonal solar system faces reference year, monthly normal, weather conditions, (2) has achieved steady state operating conditions, and (3) is capable of meeting the full heating load without auxiliary backup.[6,7] Table 1 gives the monthly normal values for degree days (which are equivalent to T_ℓ) and daily insolation on a tilted surface, H_T, for the four sites considered in this report: Caribou, Maine; Madison, Wisconsin; Boston, Massachusetts; and Sterling, Virginia.[8,9]

Although less than adequate for analysis of diurnal systems, the use of reference year monthly normal weather data provides a valid benchmark for seasonal systems. Provided storage capacities are large, seasonal systems will integrate out the short-term stochastic fluctuations in insolation and load, with system performance dependent primarily on long-run (weekly, monthly) average values. Below, we determine sizing requirements of seasonal systems that exactly meet load under reference year weather conditions. While such systems will be oversized during the mild winters, they will be undersized during the more severe winters, with a shortfall in energy delivery to load occurring during the later stages of the winter season. An analysis of alternatives available for meeting this load deficit is deferred to the following section.

Assuming the exogenous temperatures T_c and T_ℓ are periodic over the year, the corresponding periodic (steady-state) solution for T_s can be constructed directly by substituting in Eq. 14 Fourier-series representations for all temperature variables of the form

$$T_i = T_i^\circ + \sum_{n=1}^{N}\left[T_{i_1}^n \sin(n\omega t) + T_{i_2}^n \cos(n\omega t)\right] \quad , \tag{15}$$

with ω the fundamental angular frequency (2π/year). With October 1 taken as the start of the yearly cycle (just before onset of the heating season), Table 2 gives the leading Fourier-series coefficients for T_ℓ and H_T, evaluated for each site using the monthly normal data in Table 1. Using Eq. 9 the corresponding coefficients for T_c can be calculated for specific values of the collector parameters $(\tau\alpha)$ and U_c.[10]

Approximating the finite difference term $\Delta T_s/\Delta t$ by its limiting derivative dT_s/dt, Eq. 13 can be reduced to a set of algebraic equations by equating the sum of coefficients of each Fourier-series term to zero. This yields a single equation for the coefficient of the time independent term T_s°

$$T_s^\circ = \left(\lambda_c + \lambda_s\right)^{-1}\left(\lambda_s T_g + \lambda_c T_c^\circ - \lambda_\ell T_\ell^\circ\right) \quad . \tag{16}$$

and a set of coupled equations for the nth order coefficients $\{T_{s_1}^n, T_{s_2}^n\}$

$$\begin{aligned} \left(\lambda_c + \lambda_s\right)T_{s_1}^n - n\omega T_{s_2}^n &= \lambda_c T_{c_1}^n - \lambda_\ell T_{\ell_1}^n \quad , \\ n\omega T_{s_1}^n + \left(\lambda_c + \lambda_s\right)T_{s_2}^n &= \lambda_c T_{c_2}^n - \lambda_\ell T_{\ell_2}^n \quad . \end{aligned} \tag{17}$$

Equations 16 and 17 provide explicit solutions for the tank temperature coefficients. An implicit assumption in their derivation is that the parameters U_c, U_ℓ and U_s are strictly constants independent of time. While adequate for the rough treatment presented here, the value of these parameters will in fact vary over the course of the year. U_c, for example, will be larger during summer than winter by about 30% because of the greater number

Table 2. Leading Fourier Series Coefficients for T_ℓ and H[a,b]

	Location	T_ℓ^0	$T_{\ell 1}^1$	$T_{\ell 2}^1$	$T_{\ell 1}^2$	$T_{\ell 2}^2$	$T_{\ell 1}^3$	$T_{\ell 2}^3$	$T_{\ell 1}^4$	$T_{\ell 2}^4$
T_ℓ(°F)	Sterling	13.8	16.8	-5.8	-1.5	-2.7	.3	-.9	-.22	-.07
	Boston	15.5	17.2	-7.8	-1.9	-2.0	-.3	-.6	-.06	-.11
	Madison	21.3	23.1	-8.4	-1.7	-2.8	0.	-.5	-.33	-.09
	Caribou	26.5	24.3	-10.0	-1.6	-1.5	-.7	-.01	-.05	.36
		H^0	H_1^1	H_2^1	H_1^2	H_2^2	H_1^3	H_2^3	H_1^4	H_2^4
H_T(kWh/m^2/day)	Sterling	4.53	-.83	-.07	-.02	.31	.10	.04	.06	.04
	Boston	3.89	-.91	-.10	-.15	.22	.02	.14	.01	.05
	Madison	4.39	-.79	-.05	-.37	.28	.04	.13	.08	.23
	Caribou	4.38	-.71	-.71	-.73	.43	.06	.03	.14	.08

[a] Calculated from monthly normal data presented in Table 1.

[b] Start of yearly cycle is October 1.

of daylight hours in summer that causes the fraction f to increase. Although not detailed here, a more precise treatment would require Fourier-series representations for these parameters comparable to those used for the temperature variables, with the solutions for the tank temperature coefficients still reducible to algebraic equations. For this more precise approach, however, the resultant Fourier-series solutions are more complex; beyond the simplest sinusoidal expansion discussed below it is probably more efficient to directly solve Eq. 14 using a finite difference approach.

Over the year, the tank temperature T_s assumes its maximum and minimum values $\{T_{s,max}, T_{s,min}\}$ at the times $\{t^*_{max}, t^*_{min}\}$ given as solutions to the secular equation

$$dT_s/dt = \sum_{n=1}^{N} (n\omega)\left[T^n_{s_1}\cos(n\omega t^*) - T^n_{s_2}\sin(n\omega t^*)\right] = 0 \quad . \tag{18}$$

The yearly maximum and minimum values of tank temperature, given explicitly by

$$\begin{aligned} T_{s,max} &= T_s\left(t^*_{max}\right) \\ T_{s,min} &= T_s\left(t^*_{min}\right) \end{aligned} \tag{19}$$

play a key role in setting collector area and storage volume requirements. The values of these two temperature parameters are generally restricted by physical constraints within the solar system, with $T_{s,min}$ required to be high enough to provide adequate heat transfer to load and $T_{s,max}$ low enough to prevent structural damage to the storage unit. For specified values of $\{T_{s,max}, T_{s,min}\}$, and with the corresponding values of $\{t^*_{max}, t^*_{min}\}$ calculated from Eq. 8, Eqs. 19 can, as we exhibit below, be inverted to provide direct estimates of collector area and storage volume requirements in terms of the physical parameters that define the system and the exogenous temperature variables.

For the remainder of this section, we specialize results to the case where temperature variables are assumed to have a simple sinusoidal behavior at the fundamental frequency $\omega = 2\pi$/year (that is, all Fourier-series are terminated beyond n=1). The particular merit of this simple case is that one can obtain analytic relations for collector area and storage volume requirements. In general the effects of higher order harmonics have been found to be relatively minor, with the results of the "sinusoidal" case adequate for the "first-cut" feasibility analysis presented here.

The solutions to Eq. 18 for $\{t^*_{max}, t^*_{min}\}$ reduce in this case to

$$\tan \omega t^*_{max} = T^1_{s_1}/T^1_{s_2} \qquad (20)$$

$$t^*_{min} = t^*_{max} + 1/2 \text{ year},$$

with the times equally spaced at half-year intervals. The corresponding values for $\{T_{s,max}, T_{s,min}\}$ are

$$T_{s,max} = T^\circ_s + \left[T^1_{s_1} \sin\left(\omega t^*_{max}\right) + T^1_{s_2} \cos\left(\omega t^*_{max}\right)\right] \qquad (21)$$

$$T_{s,min} = T^\circ_s - \left[T^1_{s_1} \sin\left(\omega t^*_{max}\right) + T^1_{s_2} \cos\left(\omega t^*_{max}\right)\right] .$$

With substitution of Eqs. 16 and 17 for T°_s, $T^1_{s_1}$, $T^1_{s_2}$, and rearrangement, Eqs. 21 can be written

$$\overline{T} \equiv \tfrac{1}{2}\left(T_{s,max} + T_{s,min}\right) = T^\circ_s = \left(\lambda_s T_g + \lambda_c T^\circ_c - \lambda_\ell T^\circ_\ell\right) \qquad (22)$$

$$\Delta T^2 \equiv \left(T_{s,max} - T_{s,min}\right)^2 = \frac{4\left[\left(\lambda_c T^1_{c_1} - \lambda_\ell T^1_{\ell_1}\right)^2 + \left(\lambda_c T^1_{c_2} - \lambda_\ell T^1_{\ell_2}\right)^2\right]}{\left[\left(\lambda_c + \lambda_s\right)^2 + \omega^2\right]} \qquad (23)$$

These equations can be inverted to provide the following explicit relations for collector area and storage volume requirements

$$A_cU_c = \left(T_c^\circ - \bar{T}\right)^{-1}\left[A_\ell U_\ell T_\ell^\circ + A_sU_s\left(\bar{T} - T_g\right)\right] \tag{24}$$

$$V_s/A_c \doteq U_c/\omega\rho c_p \left[4\left(T_{c_1}^1 - \gamma T_{\ell_1}^1\right)^2 + 4\left(T_{c_2}^1 - \gamma T_{\ell_2}^1\right)^2 - \Delta T^2(1+\delta)^2\right]^{\frac{1}{2}}\Delta T^{-1}, \tag{25}$$

where γ, δ are the ratios $A_\ell U_\ell/A_cU_c$ and A_sU_s/A_cU_c, respectively.

Eqs. 24 and 25 are a coupled set of equations that can be solved simultaneously to provide unique solutions for A_c and V_s/A_c. These values represent minimum collector area and storage volume adequate to just meet load, under the specified constraints on the minimum and maximum tank temperature. As seen from these equations, collector area requirements depend only on the yearly average values of the exogenous temperature variables, while storage volume requirements depend upon the yearly fluctuations in temperatures. The yearly average storage temperature $\bar{T}$ affects collector area requirements directly through its effect on collection efficiency and indirectly through its effect upon storage tank losses, with A_c reduced as $\bar{T}$ is lowered. One way to reduce $\bar{T}$ without adversely affecting volume requirements is to lower $T_{s,min}$, and in what follows we assume that $T_{s,min}$ is always set at the minimum value consistent with heat transfer requirements. To reduce $\bar{T}$ and hence A_c by lowering $T_{s,max}$ also decreases ΔT and has the simultaneous effect of increasing storage volume V_s.

Within the sinusoidal approximation an explicit expression can be derived for the annual system efficiency, ε, defined as the percent of available solar energy actually transfered to load over the year

$$\varepsilon \equiv \int_{year} \dot{Q}_{load}(t)dt / \int_{year} H_T(t)dt \approx (\tau\alpha) \cdot \frac{A_\ell U_\ell}{A_c U_c} \cdot \frac{T_\ell^\circ}{(T_c^\circ - T_a^\circ)} \qquad (26)$$

Figures 3A-D and 4A-D display graphically the behavior of the solutions to Eqs. 24-26 at all four sites, giving A_c, V_s, V_s/A_c and ε as functions of ΔT for different levels of tank insulation. The specific values of the load and system parameters held constant in these calculations are listed in Table 3. One of the principal results apparent from these graphs is the pronounced effect storage tank losses have on overall system efficiency. In Figs. 3A and 4A, the difference in area requirements between a specific R-value curve and the corresponding $R = \infty$ curve represents the excess area requirements needed solely to replenish storage losses over the year. The effect can be substantial, approaching 50% additional collector area at higher values of ΔT. In order to keep storage losses (and hence additional collector area) at a manageable level, in the range of 10-20% of the total energy collected over the year, storage vessels with extremely high insulation properties are required with R values above 80.

As tank insulation improves, both collector area and storage volume requirements decrease, with the system producing a higher overall yearly efficiency. Higher tank insulation levels also decrease the ratio of storage volume to collector area, by shifting the optimum design to include more storage volume and less collector area. At the higher values of ΔT the ratio is in the relatively low range of 2-4. At the higher tank insulation levels, the overall yearly efficiency of the system is high, reflecting the high-grade collector parameters used in the calculations. The use of lower-grade collector parameters would degrade the overall system efficiency, particularly at the higher values of ΔT.

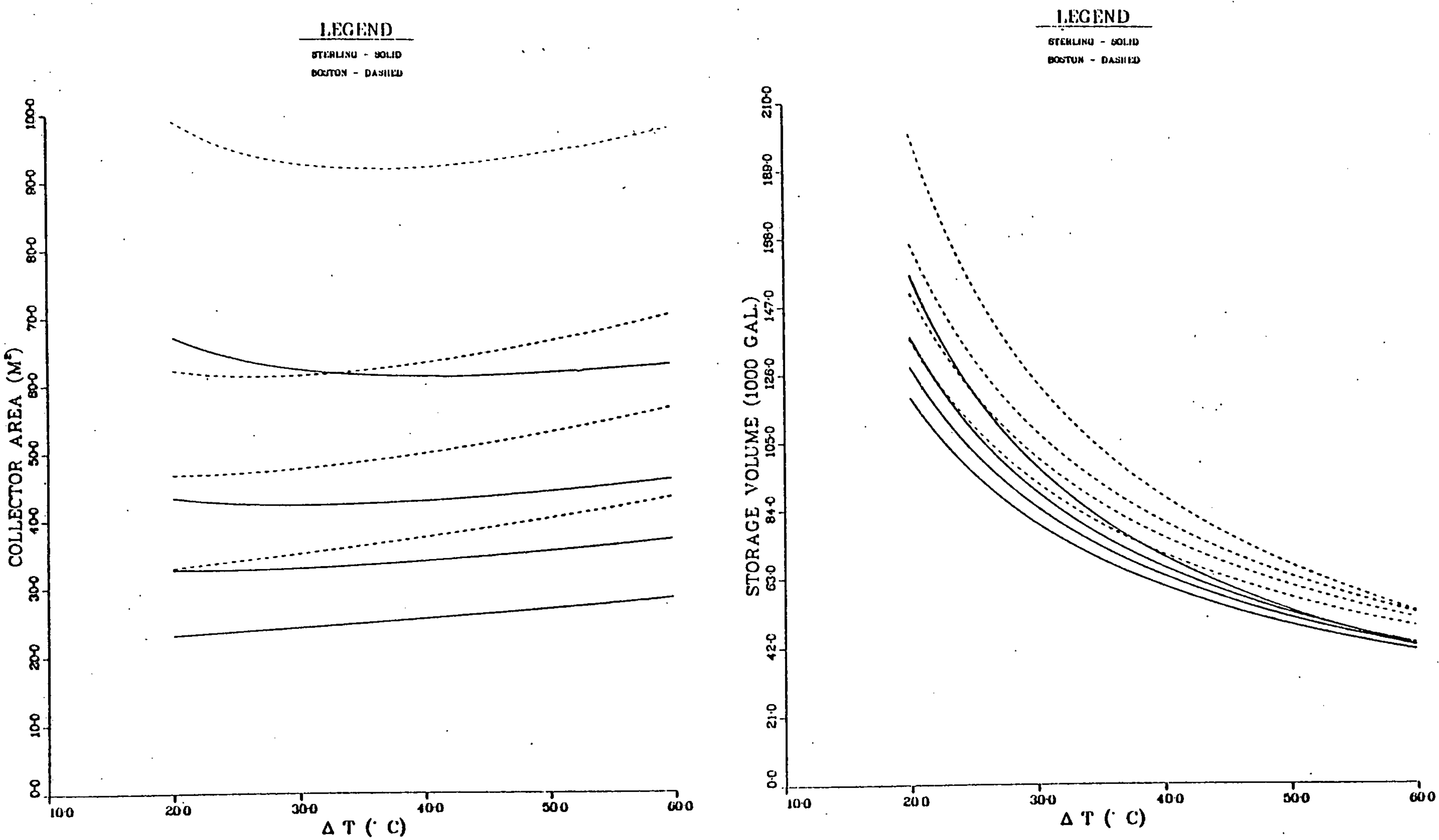

Figs. 3A-B. Collector Area and Storage Volume Requirements as a Function of Yearly ΔT. For each location, four curves are presented corresponding to different levels of tank insulation (R=20, 40, 80, ∞), with the topmost curve corresponding to R=20, and bottommost to R = ∞.

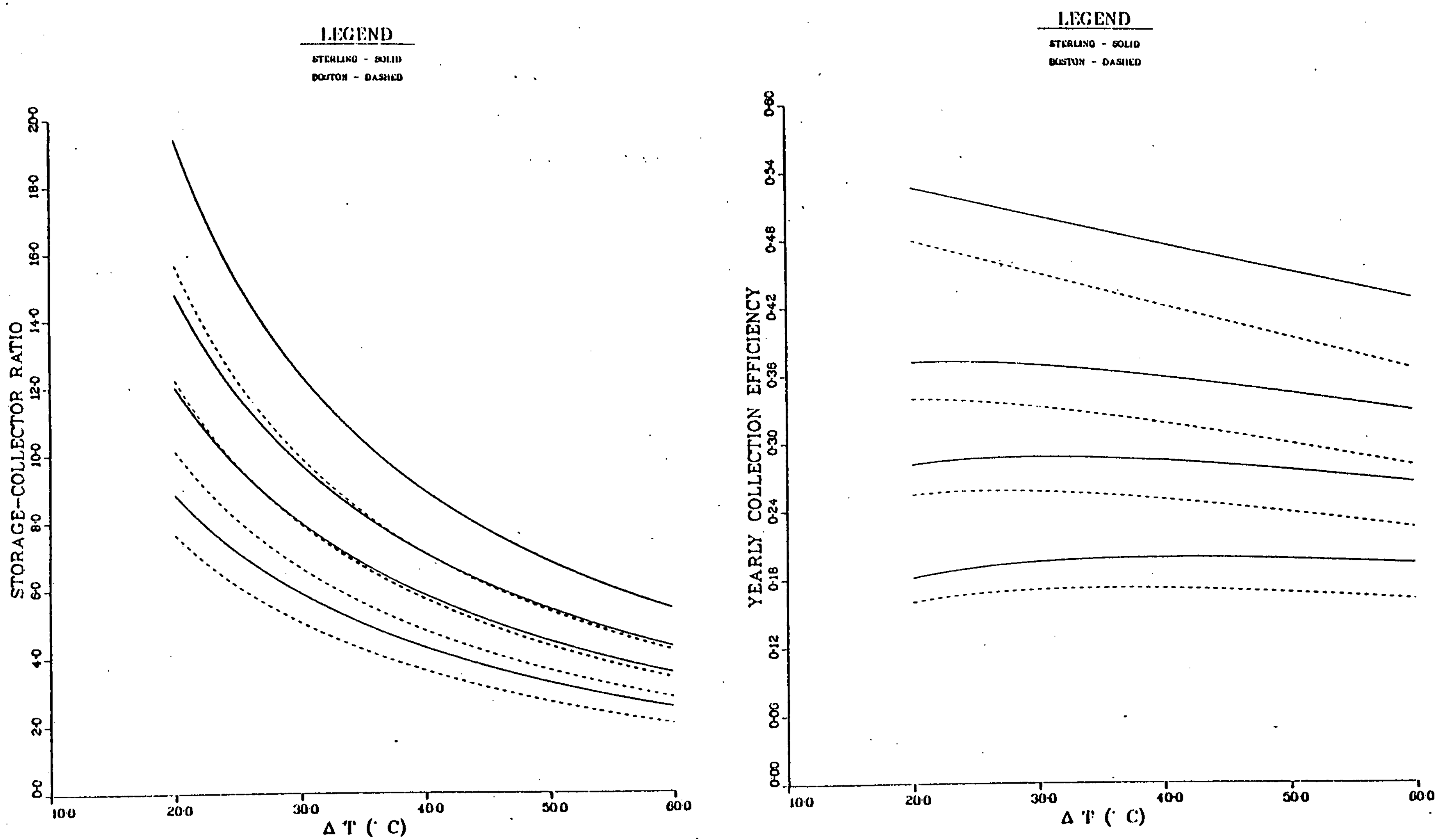

Figs. 3C-D. Storage Volume to Collector Area Ratio, and Overall System Efficiency as a Function of Yearly ΔT. At each location, the topmost curve corresponds to R = ∞, the bottommost to R = 20.

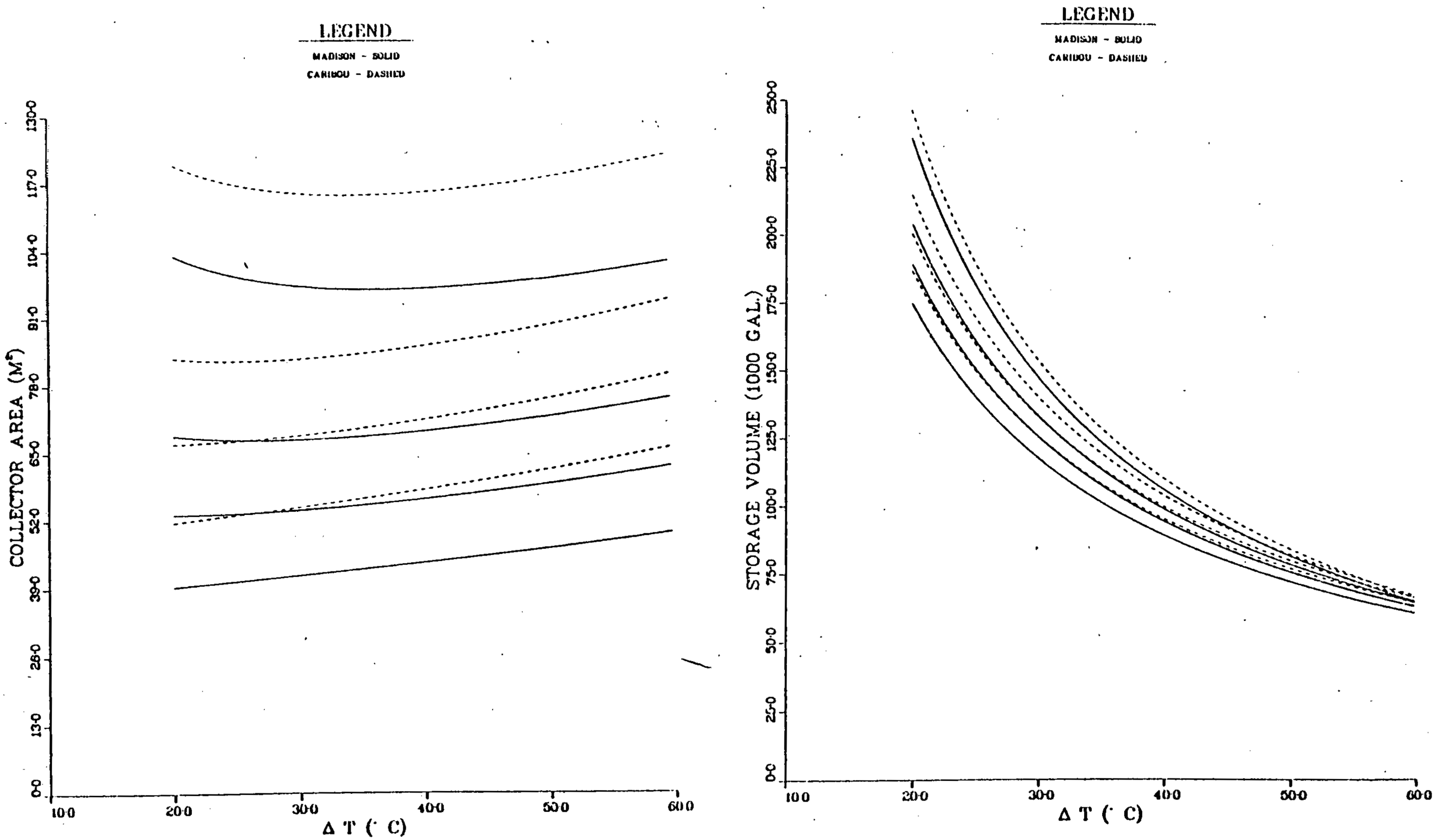

Figs. 4A-B. Collector Area and Storage Volume Requirements as a Function of Yearly ΔT. For each location, four curves are presented corresponding to different levels of tank insulation (R=20, 40, 80, ∞), with the topmost curve corresponding to R = 20, and bottommost to R = ∞.

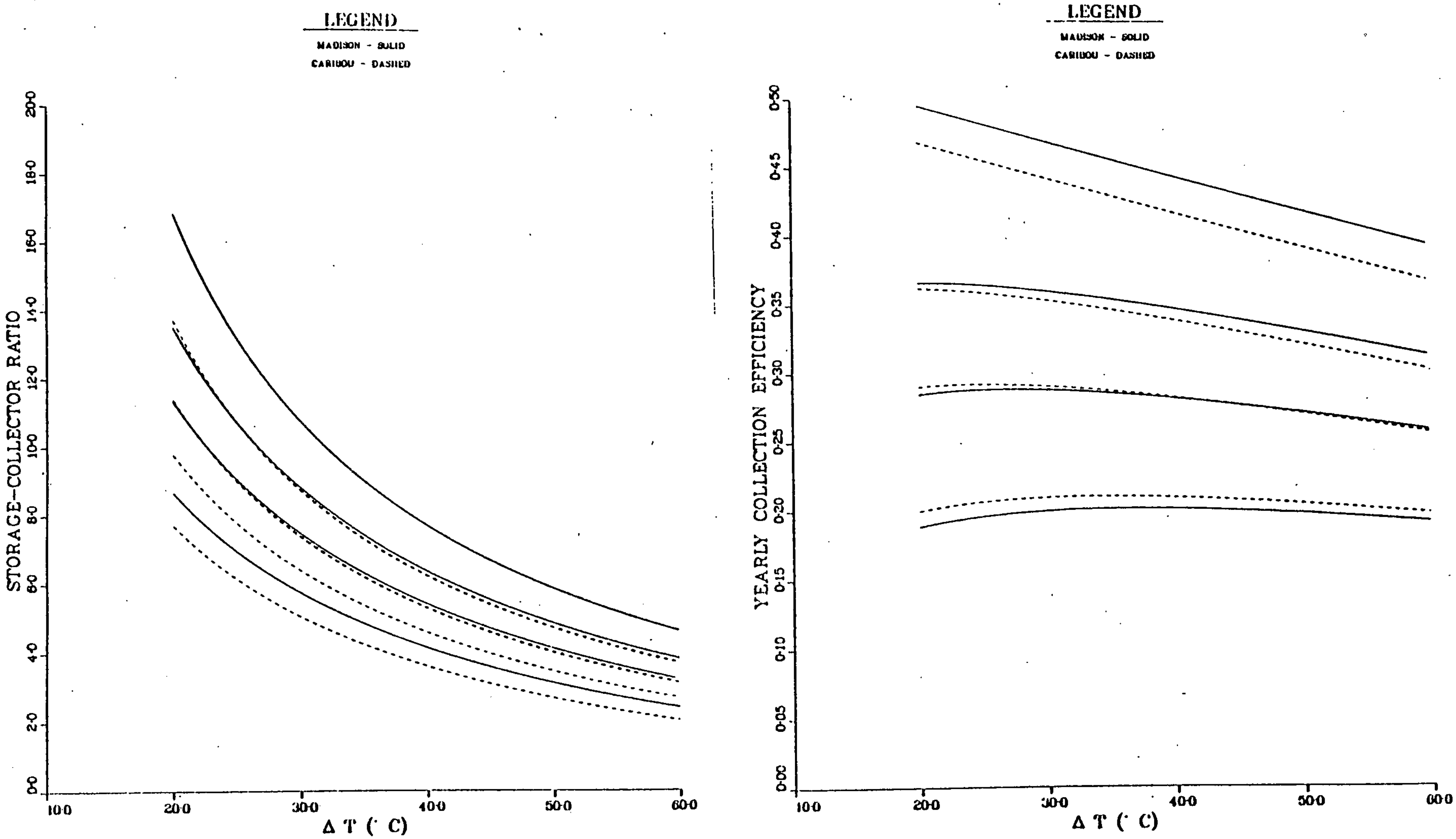

Figs. 4C–D. Storage Volume to Collector Area Ratio, and Overall System Efficiency as a Function of Yearly ΔT. At each location, the topmost curve corresponds to R = ∞, the bottommost to R = 20.

Table 3. System and Load Performance and Cost Parameters

System Parameters			
Collector			
	$F_R U_L$	kJ/m^2-°C-hr	11.
	$\tau\alpha$	dimensionless	.73
	tilt	degrees	latitude +10°.
	f	dimensionless	.33
	U_c	kJ/m^2-°C-hr	3.7
Storage			
	U_s	kJ/m^2-°C-hr	1.-0.(R=20.-∞)
	T_g	°C	13.
	ρc_p (water)	kJ/m^3-°C	4184.
Load Parameters			
	U_ℓ	kJ/m^2-°C-hr	3.
	A_ℓ	m^2	350.
	P_{max}	kJ/hr	30-50,000
	Q_L	kJ/year	80-150 × 10^6
Cost Parameters			
Real Capital Recovery Rate	i	dimensionless	.10
Levelized Fuel Factor	L	dimensionless	2
	C_{conv}	\$/kW	50
	c_F	\$/10^6 Btu	3-10
	c_c	\$/m^2	0-200

As ΔT increases, the effect on area requirements is twofold: at the lower values of ΔT the effect is to decrease A_c because of reduced storage volume hence storage losses; at the higher values of ΔT the effect is to eventually increase A_c because of greater collector inefficiencies. For the near-term range of practical values of ΔT (below 60°C) the second effect is seen to remain small for the high grade collector considered here. As ΔT increases the corresponding effect on storage volume requirements is to lower V_s, roughly as $(\Delta T)^{-1}$. In the following section we explore the economic tradeoffs between these collector area and storage volume requirements.

V. ECONOMIC ANALYSIS

In this final section we present a comparative analysis of supply costs for a seasonal solar system relative to the costs of conventional space heating systems. There are two steps to the calculations. First, we present estimates of storage breakeven costs for the seasonal solar system designs studied in the previous section. Because of considerable uncertainties in collector costs and the cost of fuel for the competing conventional system, we have parametrized break-even storage cost estimates in terms of these two cost variables. Second, we evaluate the cost impacts of design modifications required in order to insure that the seasonal solar system can reliably meet load under worst case winter conditions.

With unit collector cost denoted by c_c and unit storage cost by c_s, we express the total installed capital cost of the seasonal solar system by the simple algorithm

$$C_{sol} = c_c \cdot A_c + c_s \cdot V_s \quad . \tag{27}$$

For simplicity, the costs of pumps, pipes, controls and heat-exchangers are assumed allocated to either the collector or storage unit, and maintenance costs are neglected. Under reference year weather conditions where the seasonal solar system requires no auxiliary fuel, the annual cost of supplying space heating is obtained simply by multiplying Eq. 27 by the real capital recovery factor i.

In general, the unit storage cost parameter c_s is not a constant, but rather depends on a number of system variables including: (1) V_s, reflecting the materials of construction of the containment vessel surface area, with the dependence roughly proportional to $V_s^{-2/3}$; (2) ΔT, with the higher values of ΔT requiring improved storage materials and designs, hence higher unit costs; and (3) U_s^{-1}, the level of tank insulation. Likewise the unit collector cost c_c will depend on the collector parameter values F_R, $(\tau\alpha)$, U_L.

The comparable supply cost of a conventional fossil fuel-fired furnace is given by

$$C_{con} = c_{conv} \cdot P_{max} + c_F \cdot L\ Q_L/\eta i \quad , \tag{28}$$

where the system must be sized to the maximum heating load requirement P_{max}, and fuel requirements are set by the annual total heating load Q_L scaled up by the furnace conversion efficiency η. By equating C_{sol} to C_{con} and solving for c_s we can obtain an expression for the break-even cost of seasonal storage comparable to that given in Eq. 7.

$$\tilde{c}_s = \frac{1}{V_s}\left[c_{conv}\ P_{max} + c_F L Q_L/\eta i - c_c A_c\right] \quad . \tag{29}$$

In what follows we attempt to show the dependence of $\tilde{c}_s$ on the major system parameters specified in Eq. 29. It is important to emphasize, however, that these dependencies in $\tilde{c}_s$ are in no way related to those in the parameter c_s. $\tilde{c}_s$ represents the maximum acceptable cost of storage, while c_s represents actual cost.

Figures 5A-D illustrate for all four sites the behavior of $\tilde{c}_s$, calculated for the corresponding A_c, V_s values derived in the previous section (and shown in Figs. 3, 4A-D). The cost parameters in Eq. 29 were fixed within the ranges given in Table 3, with c_c at \$100/m^2 and c_F at \$3/10^6 Btu. While the storage break-even costs increase substantially with ΔT at the higher values of tank insulation, they quickly saturate for the less well insulated tanks, reflecting the lower economic utility of these systems. In these systems a large fraction of

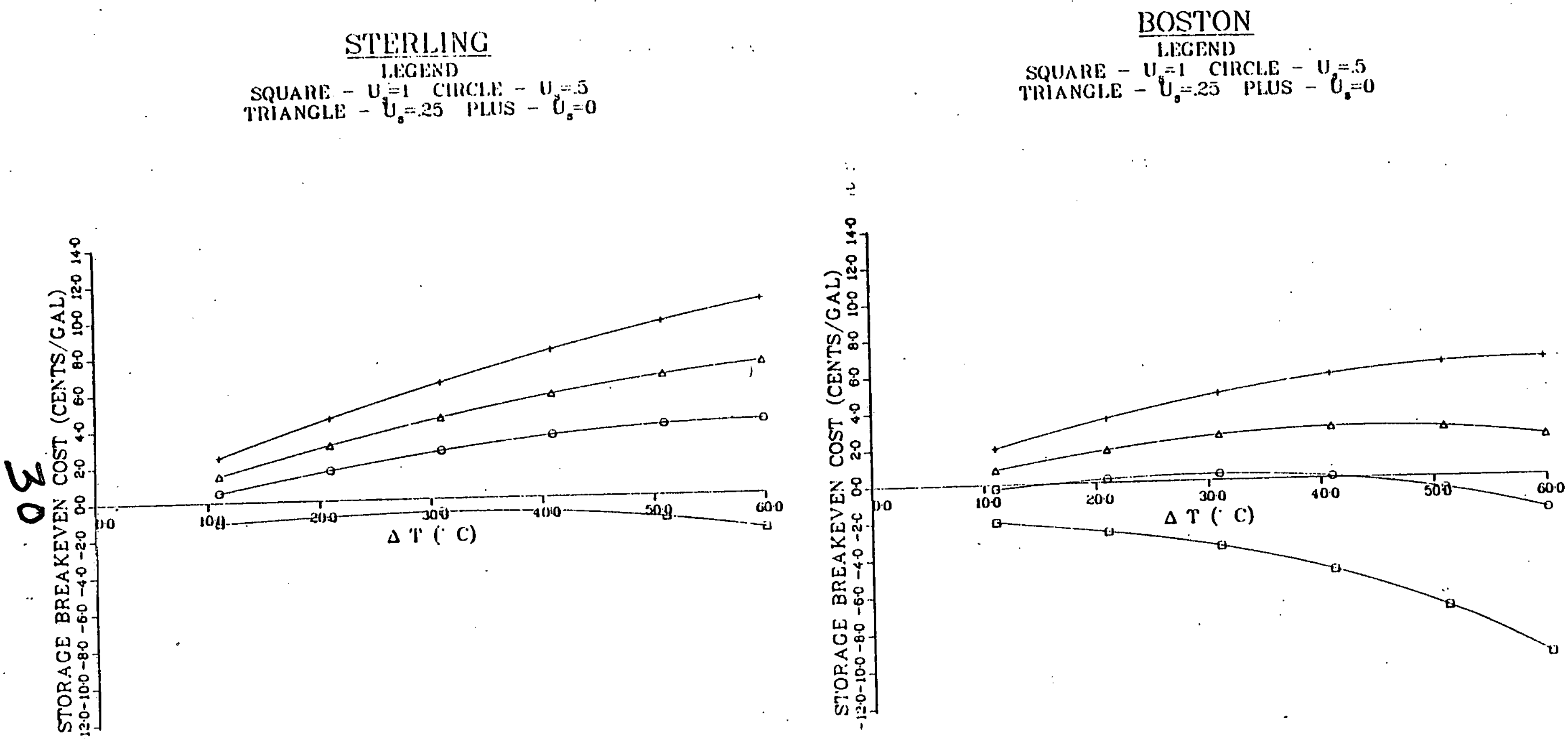

Figs. 5A-B. Estimated Storage Break-Even Costs as a Function of Yearly ΔT, for Four Levels of Tank Insulation. In three calculations collector costs were taken at $\$100/m^2$, and levelized conventional fuel costs at $\$6/10^6$ Btu.

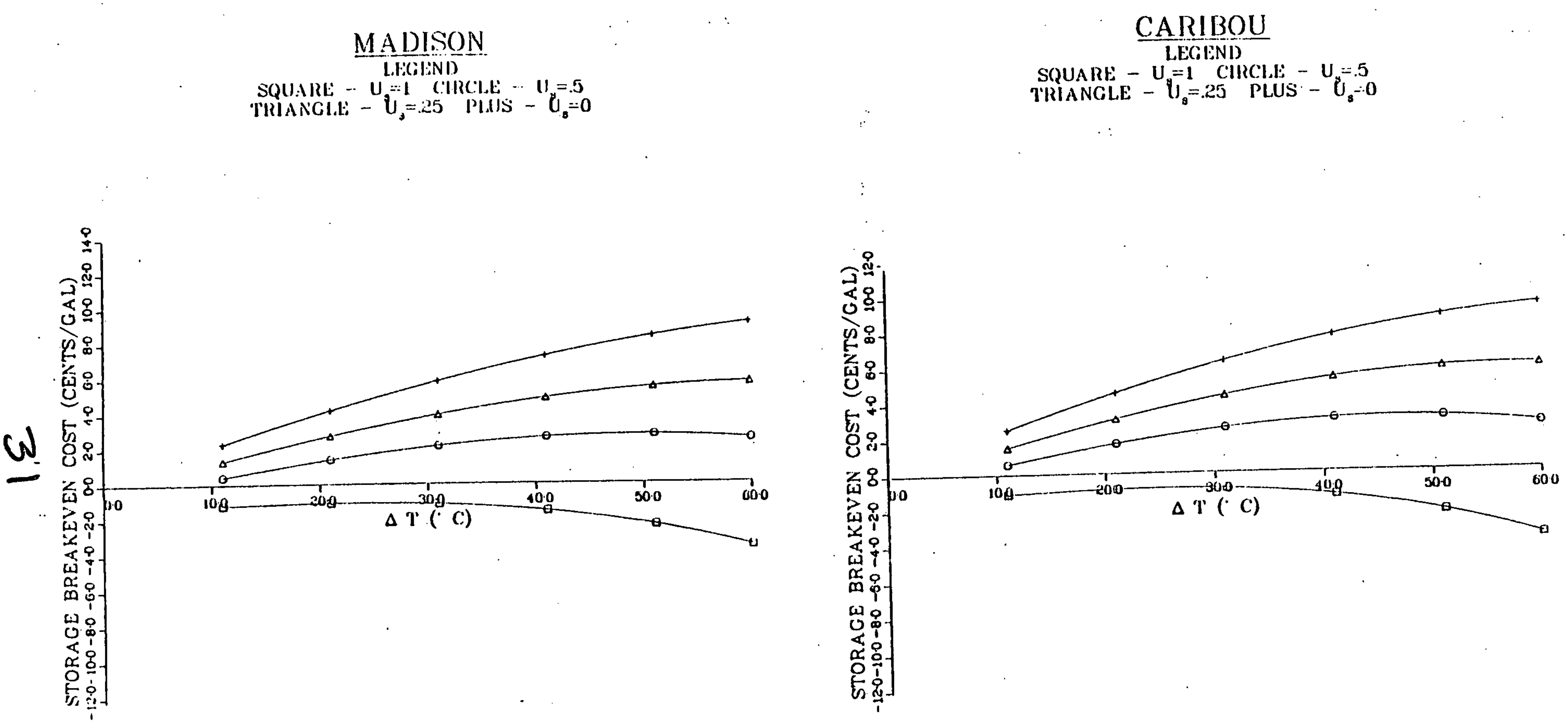

Figs. 5C-D. Estimated Storage Break-Even Costs as a Function of Yearly ΔT, for Four Levels of Tank Insulation. In three calculations collector costs were takn at $\$100/m^2$, and levelized conventional fuel costs at $\$6/10^6$ Btu.

the collected energy is lost during the course of the year. For non-zero collector costs the values of $\tilde{c}_s$ will eventually drop to zero at sufficiently high values of ΔT where collector area-related costs become comparable to the conventional system costs.

As the final topic in this section we consider the alternatives available for meeting load under worst case winter conditions. Table 4 provides a summary description of the statistical variation in both yearly heating degree days and yearly insolation levels observed at each site over the last several decades. While the seasonal solar designs specified in the previous sections will meet the entire load during winters milder than the reference year they will fall short during winters more severe than the reference year. The alternatives we consider for making up this load deficit are to oversize the solar system or incorporate a small auxiliary backup system. Although not explicitly considered here, one important factor favoring the need for an auxiliary backup occurs during the initial startup period for the system when it will not be fully charged, requiring greater than normal levels of backup energy.

The required oversizing of the seasonal solar system is calculated here under the following assumptions: (1) the relative sizing of collector area to storage volume remains constant at the value calculated for the reference year; (2) system efficiency remains constant; (3) systems are oversized to meet a 2-standard deviation in winter conditions or a 1 in 20 year outage probability (95% reliability); and (4) there is no thermal carry-over from year to year, a reasonable approximatation because during late summer - early fall the collectors largely feed the parasitic losses. For the

Table 4. Statistical Analyses of Yearly Degree Days and Insolation[a]

Location	Observation Period	Annual Degree Days[b]					Annual Insolation (10^6 kJ/m^2)[c]			
		Mean	St. Dev.	Max.	Min.	TILT	Mean	St. Dev.	Max.	Min.
Madison	1953-75	7454.	404.	8424.	6662	53°	6.09	.24	6.43	5.71
Sterling	1953-75	4795.	418.	5517.	4084.	45°	5.97	.23	6.59	5.61
Boston	1953-68	5816.	400.	6312.	4943.	53°	5.60	.23	5.91	5.23
Caribou	1953-75[d]	9425.	395.	10000	8539	53°	5.61	.26	5.91	5.10

[a] Derived from Solmet hourly data base, available from National Climatic Center, Asheville, N.C.

[b] Calculated from daily average temperatures (base 65°F).

[c] Calculated global radiation received on a tilted surface.

[d] Exclusive of years 1961, 63, 67, 68, 73, 74 for which there were gaps in insolation data.

reference year and more milder winters we have the following inequality between system output and load requirements

$$0 \leq g \equiv A_c \varepsilon \langle H_T \rangle_{year} - \langle Q_L \rangle_{year} \quad , \tag{30}$$

where <> refers to yearly totals and A_c and ε are the values calculated in the previous section. Assuming no correlation between yearly insolation and degree days, the percent increase in A_c required to maintain Inequality (30) under a 2-standard deviation in winter conditions, that is to maintain the inequality $g - 2\sigma_g \geq 0$, is

$$A_c'/A_c = \frac{1 - \sqrt{1 - \left(1 - 4\sigma_{H_T}^2/\bar{H}_T^2\right)\left(1 - 4\sigma_{Q_L}^2/\bar{Q}_L^2\right)}}{\left(1 - 4\sigma_{H_T}^2/\bar{H}_T^2\right)} \quad . \tag{31}$$

where $\overline{X}$, σ_X refer to average value and standard deviation, respectively. For the data in Table 4 the percentage increases vary from 5-10% for all four sites.

Assuming the seasonal systems are just cost competitive with the conventional systems under reference year weather conditions, a 5-10% increase in capital cost for the seasonal solar system required to meet worst case winter conditions appears to be well above the cost of a small auxiliary backup device plus auxiliary fuel requirements. Because the available storage capacity of the system can be used to smooth out load patterns, the auxiliary backup can be sized well down from the design requirements of conventional systems, and hence be of lower cost.

The general result of this report has been to develop a simplified model useful for studying collector and storage sizing and design requirements. While the application of this model has shown substantial performance gains for the seasonal over a comparable diurnal system, the corresponding storage break-even costs remain relatively low.

REFERENCES

1. See, for example, F.C. Hooper and C.R. Attwater, "Optimization of an Annual Storage Solar Heating System over its Life Cycle," presented at International Solar Energy Society Meeting, American Section, Orlando, Florida, June 1977.

2. The complexities, and comparative costs, of augmenting diurnal solar heating systems by electric, oil or natural gas backup systems have been discussed in a number of recent papers. See (1) J.G. Asbury and R.O. Mueller, "Solar Energy and Electric Utilities: Should They Be Interfaced?," Science 195, 445 (February 1977); (2) J.G. Asbury, R.F. Giese, and R.O. Mueller, "The Interface with Solar: Alternative Auxiliary Supply Systems," Proceedings of the International Solar Energy Society Meeting, New Delhi, India, Jan. 1978.

3. In this comparison the cost of storage for the diurnal system is neglected.

4. The analysis presented here neglects the performance gains possible with heat stratification in the tank, as well as through controlled valving alternatives that permit direct transfer of heat between collector and load during the winter heating season. Although these effects will improve overall system performance, perhaps substantially under some circumstances, they are not expected to invalidate the qualitative sizing and cost conclusions reached here. For a discussion of stratification effects in diurnal solar systems, see D.W. Connor and R.O. Mueller, "The Effect of Stratified Heat Storage on Overall Heat Transfer in Solar Heating Systems," ANL report, forthcoming.

5. Valid in a steady state, this approach neglects transient effects caused by heating and cooling of the surrounding earth.

6. Although not considered here, an analysis of partial seasonal solar systems supplemented by an auxiliary energy backup could proceed directly from Eq. 14.

7. During the start-up period, extending into the first operating season, the system is likely not to be fully charged and hence will underperform, requiring a supplemental energy source. This initial value problem is not considered explicitly in the present analysis.

8. Climatological data obtained from the National Climatic Center, Asheville, N.C. See Table 1 for specific citations to data sources.

9. In the present analysis, collector tilt was taken to be latitude +10°. Because of collector and storage losses the value of a collected Btu increases with its proximity in time with the winter heating season, implying tilts that favor the winter season for seasonal systems.

10. For simplicity, we approximate $\langle T_a \rangle_c$ in Eq. 9 by the daily average values.